Comparative study of Cu-impregnated ZnO and Ag-impregnated ZnO visible light driven photocatalysts for the sonophotocatalytic degradation of cefpodoxime proxetil in aqueous solution

Fatima Khitab[a,b,*], Jasmin Shah[b], Muhammad Rasul Jan[b]

[a]*Department of Chemistry, Shaheed Benazir Bhutto Women University, Peshawar 25000, Pakistan,*
email: Fatima_khitab@yahoo.com (F. Khitab)
[b]*Institute of Chemical Sciences, University of Peshawar, Peshawar 25000, Khyber Pakhtunkhwa, Pakistan*

ABSTRACT

A comparative study of Cu-impregnated ZnO and Ag-impregnated ZnO for the sonophotocatalytic degradation of cefpodoxime proxetil in aqueous solution under visible light irradiation were carried out. Optimum conditions for degradation of cefpodoxime proxetil using Cu-ZnO and Ag-ZnO was investigated. The effect of enhancers and scavengers were investigated using optimum conditions and hydrogen peroxide as enhancers. 100% degradation was achieved using Cu-ZnO and Ag-ZnO. Furthermore, total organic carbon analysis was carried out and 89% using Cu-ZnO and 93% using Ag-ZnO removal of total organic compounds were observed. The sonophotocatalytic degradation of cefpodoxime proxetil using Cu-ZnO and Ag-ZnO followed pseudo-first-order kinetic and the rate of degradation of cefpodoxime proxetil using Ag-ZnO was found higher (k_1 = 0.228) than the Cu-ZnO photocatalyst (k_1 = 0.185). The method has also been successfully applied in samples for sonophotocatalytic degradation.

Keywords: Sonophotocatalysis; Impregnated ZnO; Cefpodoxime proxetil; Degradation; Regeneration

1. Introduction

Antibiotics are used to treat and prevent epidemic diseases in human's animals and plants. Antibiotics are natural, semi-synthesized or synthesized complexes with antimicrobial action [1,2]. Antibiotics are disposed often into the sewage system in the form of unused drugs or the metabolized [3]. Todays the increasing presence of drugs in the environment is a national and international problem [4]. Although the concentrations of pharmaceuticals in the environment may be very low but sufficient to have adverse effects on the environment and humans [5]. Long-term exposure to traces and mixtures of pharmaceuticals can affect the vulnerable population, including pregnant women, newborns, and children [6]. If the drugs are not degraded or eliminated during the treatment or any other usage, they will reach surface and ground water and possibly drinking water [7,8]. The widespread use of the drug substance is worrisome to human health, not only in terms of the spread of resistant bacteria, but also for other natural damage. Most pharmaceutical companies and hospitals do not have treatment facilities to remove antibiotics and other pharmaceutical compounds from their wastewater [9,10]. Typically, wastewater from pharmaceutical companies and hospitals is discharged directly into the sewage system, which in turn enters the canals used for crop irrigation. On the other hand, a certain quantity of sewage reaches the ponds of stagnant water. These ponds are also a source of drinking water for animals. Aquatic life affects most of this habit. Due to shortcomings of photocatalytic technique

* Corresponding author.

such as long reaction time, [11] the immediate need is to develop a simple, economical, reproducible, and accurate method for the degradation of residual antibiotic levels in these samples [12,13]. From our previous research ultrasonic-assisted photocatalytic technique was found to be a very promising technique for the degradation of organic pollutants therefore for the degradation of cefpodoxime proxetil sonophotocatalytic technique was used [14–16].

High photosensitivity, good stability, low cost, and non-toxicity have made ZnO photocatalyst widely used for photocatalytic degradation of various organic pollutants [17]. Despite all the characteristics and features which made metal oxide semiconductors a very useful heterogeneous photocatalysts, there are some drawbacks also [18], such as the rapid recombination rate of the generated electron–hole pairs [19] high tendency to agglomeration [20] using conventional methods difficulty in centrifugation [21] as well as low volume to surface ratio [22]. Catalytic activity can be further enhanced with doping or impregnation of metal ions, as the transition metal cations in ZnO can alter the coordination environment of Zn in the lattice [23]. ZnO have been modified with different non-metals doping [24] metal doped [25] also modified with different rare earth metals [26–28], addition of transition metals [29–31] as well as use of different coupled semiconductors [32,33].

Therefore, ZnO was modified with transition metal cations to increase its photocatalytic activity by trapping sites to decrease the rate of electron-hole recombination and to increase the photocatalytic activity and a possible way to shift the photosensitive response of ZnO to the visible region [34,35]. Interest was to prepare a photocatalysts having band gap in visible region. Semiconductors ZnO photocatalyst was impregnated with copper (Cu-ZnO) and Silver (Ag-ZnO) to increase the catalytic performance of ZnO in the visible region of spectrum with the aim to decrease the degradation time by combination with ultrasonic waves impregnation of Cu and Ag on ZnO shifts the band gap from UV to visible region. Furthermore, silver was selected because of low cost as compared to other noble metals and superior antimicrobial activities making it beneficial for the wastewater treatment. Many researchers reported impregnation of Cu and Ag to reduce charge transfer recombination effect [23]. From the best of our knowledge Cu-ZnO and Ag-ZnO is reporting first time for the sonophotocatalytic degradation of cefpodoxime proxetil.

2. Experimental

2.1. Materials and methods

All chemicals used were of analytical grade purity and used without further purification. Zinc oxide (ZnO) and copper chloride hydrated (CuCl$_2$·2H$_2$O) and silver nitrate (Ag(NO$_3$)$_2$) were purchased from BDH Laboratory Supplies, Poole, BH151TD, England. Standard references of drugs were provided by Cirin Pharmaceutical (Pvt) Ltd., Hatter, Pakistan. Commercial formulations of cefpodoxime proxetil (molecular formula = C$_{15}$H$_{17}$N$_5$O$_6$S$_2$, molecular weight = 427.458 g mol^{-1}, λ_{max} = 240 nm) magnetic caps 400 mg, S J & G Fazal Elahi (Pvt) Ltd. Darmstadt. Britton Robinson buffer was used to adjusted pH of the dyes.

2.2. Instrumentation

UV/Vis Spectrophotometer (Model SP-3000 plus, Optima, Japan), with matched 1 cm quartz cells was used for absorbance measurement at maximum wavelength of cefpodoxime proxetil (240 nm). Kum Sung ultrasonic bath with 40 KH frequencies was used as ultrasonic radiation source. Tungsten filament lamp of 200 W was used as a visible source for photocatalytic degradation of drugs.

Surface morphology of ZnO and impregnated Cu-ZnO, Ag-ZnO was analysed by scanning electron microscopy (SEM) using JSM5910 (JEOL, Japan). The specimens for SEM analysis were prepared by coating the samples with a thin layer using double adhesive carbon tape over aluminium stubs. The surface area was determined by a surface area analyser (Quanta chrome, Nova Station, A) with nitrogen adsorption–desorption isotherms. The samples were out gassed prior to analysis at 100°C for 2 h using high vacuum line to remove all the adsorbed moisture or gases from the catalyst surface and pores. The surface area of the sample was calculated using the Brunauer–Emmett–Teller (BET) method. Phase analysis was carried out with an X-ray diffractometer (JEOL model JDX-9C, Japan) at room temperature, using monochromatic Cu-Kα radiation (λ = 1.5418 Å) at 40 KV and 30 mA in the 2θ range of 10°–80° with 1.03°/min. Total organic carbon (TOC)-VCPH analyzer (Shimadzu Co., Japan) were used for the measurement of contents of TOC.

Magnetic stirrer XMTD-702 was used for stirring. Measurement of pH was done by pH meter (Model-7020 Kent Industrial Measurement Limited Electronic Instrument LTD, Chertsey Survey England). The solutions were centrifuged on Lab electric centrifuge machine (timer 0–60 min) 0–4,000 rpm cap: 20 mL × 6 (800-1).

2.3. Photocatalyst preparation

Wet impregnation method was used to prepared metals impregnated catalysts over zinc oxide (ZnO) support following the procedure reported in our former paper [15]. 3% of AgNO$_3$ solutions were prepared and added drop wise into the slurry of 97% ZnO and stirred for 1 h at 60°C at 900 rpm. The catalyst was dried in an oven for 12 h and calcined in a furnace at 500°C for 4 h. The calcined material was crushed and passed by mesh size of 150 μm, same procedure was applied for the preparation of Cu-ZnO. 3% of Cu (NO$_3$)$_2$ salt was added into the slurry of 97% ZnO solution. ZnO slurry was prepared by using a 50% distilled water to make it creamy consistency. The mixture was stirred for 1 h and dehydrated at 120°C for 12 h. After dehydration the sample was calcined in a furnace at 500°C for 4 h. The dried sample was ground to powder and screened to a particle size ≤150 μm. Impregnation of very low quantity of metal ions, that is, 3% of copper and silver impregnation on ZnO using a wet impregnation method is the novelty of present work.

We were interested to prepare a photocatalyst that has excitation energy in a visible EMR region. Impregnation of metals like Cu and Ag with ZnO shifted band gap to visible region. To shift ZnO band gap energy to visible region research study was carried out in different conditions

which confirmed the conversion of energy gap to visible region (Fig. 1) shows that ZnO in presence of UV light show decrease in absorbance, while in case of visible light no decrease in absorbance take place because ZnO band gap is in UV region. Cu-ZnO and Ag-ZnO shows a little decrease in absorbance in presence of UV light, it must be because of ZnO while in presence of visible light it shows a maximum decrease in absorbance, which confirms the shift in a band gap from UV to visible region. The performance of both catalysts were same in visible region, although Cu-ZnO shows little more increase in performance as compared to Ag-ZnO.

2.4. Sonophotocatalytic study

In a typical experiment 100 mL flask a known concentration of cefpodoxime proxetil with optimized catalyst weight (ZnO, Cu-ZnO and Ag-ZnO) were taken in a photoreactor. The suspension in the photoreactor was placed in the dark for 30 min to ensure the establishment of adsorption–desorption equilibrium of the cefpodoxime proxetil on the surface of ZnO, Cu-ZnO and Ag-ZnO and then placed under tungsten filament lamp in sonicator applying 40 KH frequencies of ultrasonic radiations for 1 h at optimized pH and oxidizing agent. The intensity of radiations for 200 W was measured using digital lux meter and the average light intensity was 3,205 Lux. At optimized time 5 mL was taken from this solution and diluted up to 25 mL (10 μg mL^{-1}) with distilled water. For obtaining a clear solution the sample was centrifuge at 900 rpm of centrifuge machine for 30–45 min. 30–45 min was a maximum time for obtaining a clear solution. Absorbance was noted at maximum wavelength of cefpodoxime proxetil (λ = 240). Degradation was calculated using the following equation.

$$\text{Degradation} = \frac{C_o - C_f}{C_o} \times 100 \qquad (1)$$

where C_o and C_f is the initial and final concentration of drug solutions after irradiation at time t. Triplicate analysis were carried out for all the experiments. The degradation conditions were investigated by varying pH, time, catalyst weight, oxidizing agent, radical scavenger, and initial
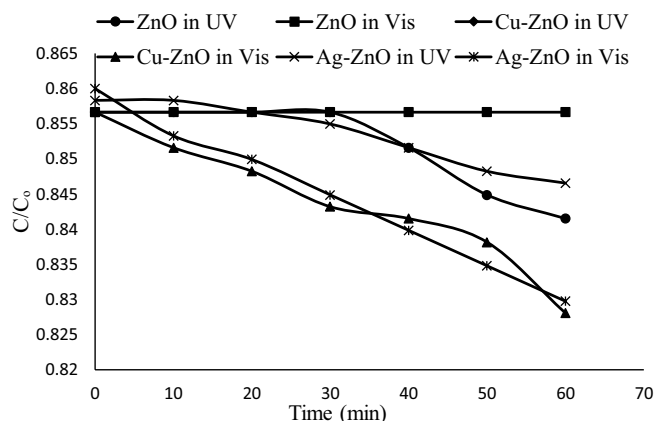

Fig. 1. Degradation of cefpodoxime proxetil using ZnO, Cu-ZnO and Ag-ZnO in UV and visible light sources.

drug concentration under sonophotocatalytic degradation. TOC analyses were carried out for the real pharmaceutical wastewater before and after sonophotocatalytic reaction to evaluate the feasibility of this process in the industry and % removal of TOC was determined by using equation also reported in our previous work [36].

$$\text{TOC\% removal} = \frac{\text{TOC}C_o - \text{TOC}C_f}{\text{TOC}C_o} \times 100 \qquad (2)$$

where $\text{TOC}C_o$ and $\text{TOC}C_f$ is the initial and final concentration mg L^{-1} of drug solutions after irradiation at time t.

3. Results and discussion

3.1. Catalyst characterization

The prepared catalysts were characterized using SEM, energy-dispersive X-ray spectroscopy (EDX), X-ray diffraction (XRD) and surface area analyser. SEM analysis confirmed that the copper and silver after impregnation was effectively dispersed throughout the surface of ZnO. The morphology of ZnO, Cu-ZnO, Ag-ZnO, reused Cu-ZnO, Ag-ZnO and reused after treatment Cu-ZnO, Ag-ZnO are depicted in Fig. 2. The impregnation of Cu on ZnO was confirmed from small rods shaped particles present on Fig. 2b (Cu-ZnO), oval shape small particles appearance on surface of Ag-ZnO confirms impregnation of silver (c) Ag-ZnO, as these particles are not present on ZnO.

The EDX spectra for ZnO, Cu-ZnO, Ag-ZnO, reused Cu-ZnO, Ag-ZnO and reused after treatment Cu-ZnO, Ag-ZnO are given in Fig. 3. The EDX spectra of Fig. 3b shows that copper and silver is successfully impregnated on ZnO while Fig. 3c shows the concentration of copper after three times repeatedly use of Cu-ZnO catalyst for photocatalytic degradation. The change in concentration of copper is negligible. Ag-ZnO re-used is also shown in Fig. 3e. The change in concentration of silver after three time reused is negligible.

Surface area was determined using BET method and it was found 182.27 m^2 g^{-1} for ZnO, 185.73 m^2 g^{-1} for Cu-ZnO and 183.73 m^2 g^{-1} for Ag-ZnO (Table 1).

The XRD of ZnO, Ag-ZnO and three cycles used Ag-ZnO, Cu-ZnO and reused Cu-ZnO is shown in Fig. 4. Height, area of the peak and their respective thickness calculated by the Scheerrer's equation for ZnO, Ag-ZnO, and three cycles reused Ag-ZnO and it was observed that 2θ values for major reflections ranges from 28° to 69° in case of ZnO, Ag-ZnO, reused Ag-ZnO. The thicknesses of the crystal lattice demonstrate that crystal thickness ranges from 17.8 to 44.8 nm for ZnO, 20.6 to 61.9 nm of Ag-ZnO and 12.2 to 35.5 nm for reused Ag-ZnO. ZnO and its pattern according to ICDD number 11136, 30888, 361451 and 11244 shows peak at 28°, 31°, 32°, 34°, 36°, 47°, 50°, 56°, 62°, 66°, 67° and 69° while b is of Ag-ZnO and it shows pattern according to ICCD number 11136, 30888, 40783 and 361451, whereas Ag shows peak at 36° and 45° Cu-ZnO shows pattern according to ICCD number 11136, 30879, 30981, 50661 and 50664 where as Cu shows peak at 43.6°, 50.7° and 74.4°, (e) of reused Cu-ZnO, it shows pattern at ICDD number 11117, 11136, 30884, 30888, 250322, 410254, 450912
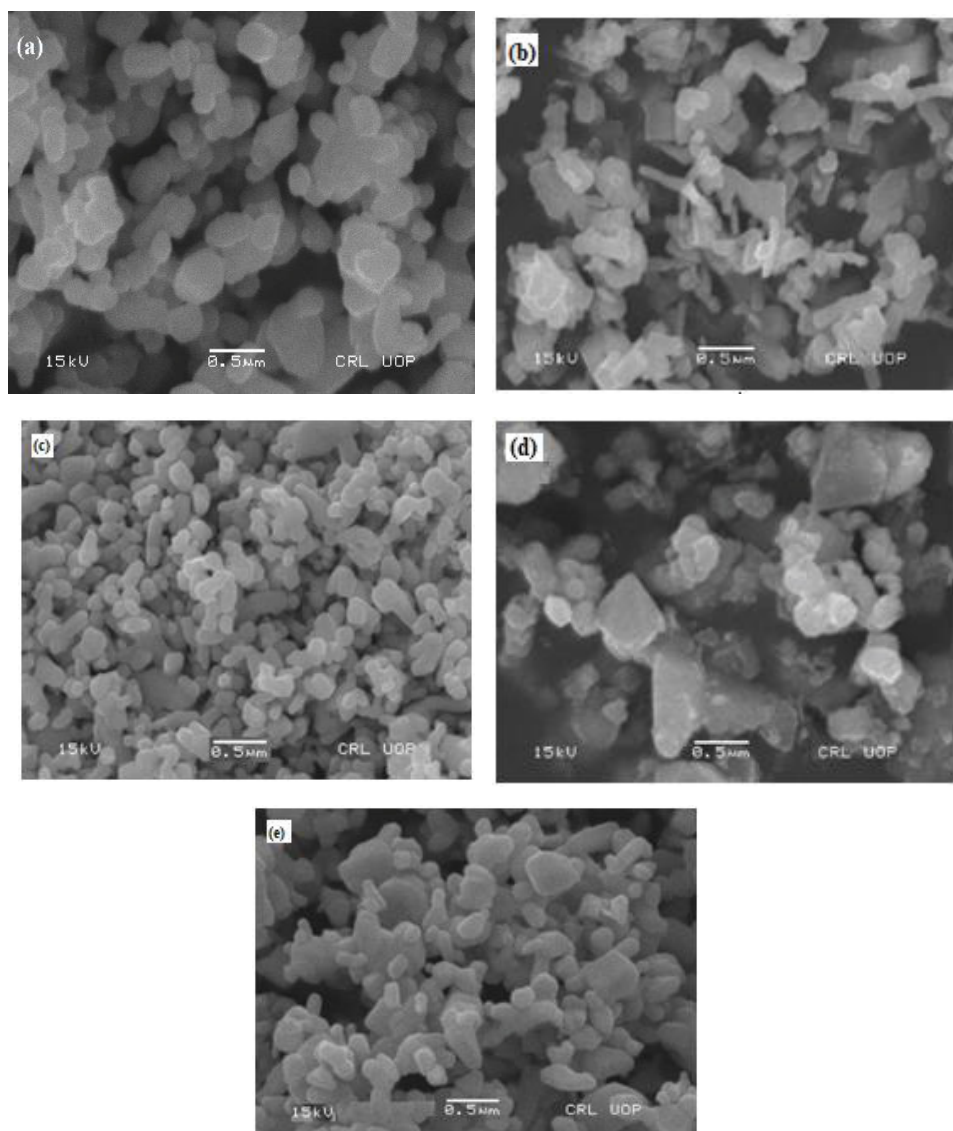
Fig. 2. SEM of (a) ZnO, (b) Cu-ZnO, (c) Ag-ZnO, (d) reused Cu-ZnO and (e) reused Ag-ZnO.

and 501381. By applying Bragg's law particle to particle distance (*d*) was found to be in the range of 0.271 to 0.63 nm for both ZnO and Ag-ZnO while it reused from 0.254 to 0.63 nm for reused Cu-ZnO. In Fig. 4 the corresponding peaks at angle >30° show residue peaks that might have been absorbed from any residue present in water.

3.2. Photocatalytic activity

The optical properties of ZnO, Cu-ZnO and Ag-ZnO were determined, and the results show that Copper and silver impregnation shift the band gap energy from UV (ZnO = 3.3 eV) to visible region (Cu-ZnO = 2.6 eV) (Ag-ZnO = 2.3 eV). The results revealed that the band gap decreased between the valence band and conduction band of ZnO after impregnation with copper and silver and lead in absorption of wide band of visible region is due to LSPR localized surface plasmonic resonance. The promotional

Table 1
Surface area, pore volume and pore size of ZnO, (Cu-ZnO, Ni-ZnO)

Sample	Method	Surface areas ($m^2 \, g^{-1}$)	Pore volume ($cc \, g^{-1}$)	Pore size (Å)
ZnO	BET	182.27	1.43	112.02
Cu-ZnO		185.73	1.43	113.07
Ag-ZnO		183.73	1.42	113.02

effect of photocatalysts after impregnation in visible light is due to consecutive electron transfer from valence band of Cu and Ag to the valence band of ZnO (Fig. 5).

To investigate the degradation of cefpodoxime proxetil, various solutions were operated with different conditions like photolysis, photocatalysis, sonolysis, sonocatalysis, and
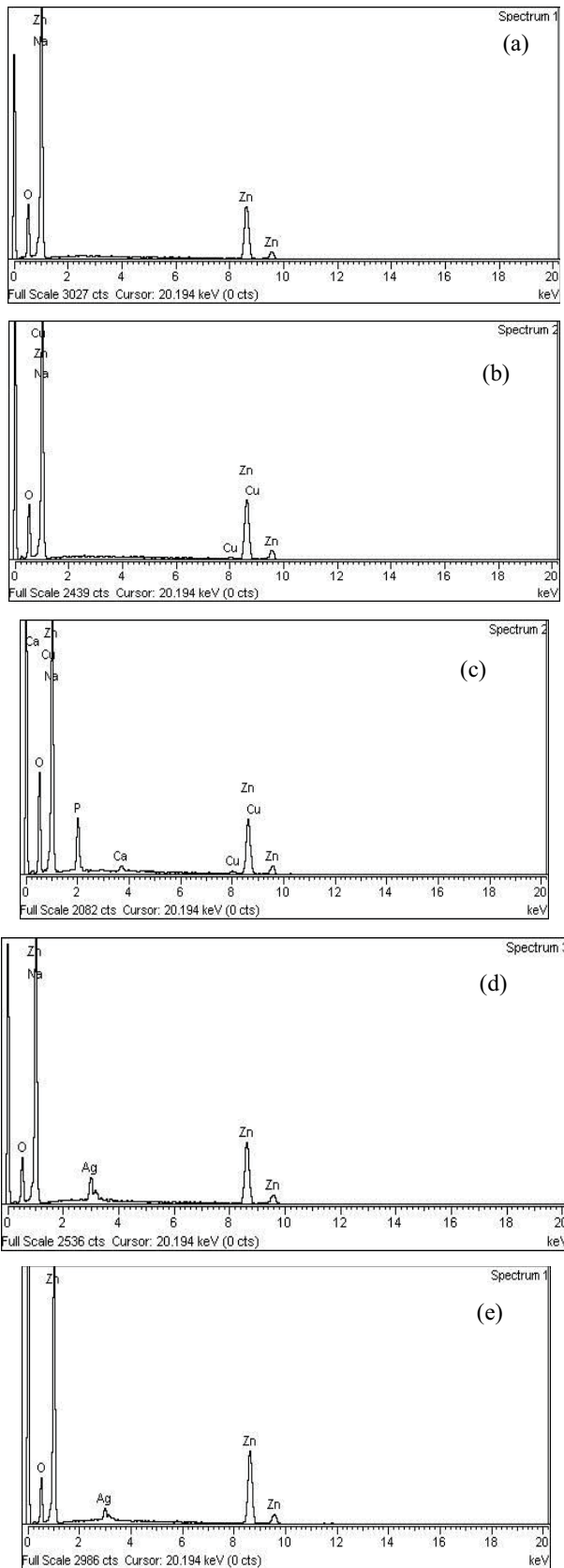
Fig. 3. EDX of (a) ZnO, (b) Cu-ZnO, (c) reused Cu-ZnO, (d) Ag-ZnO and (e) reused Ag-ZnO.
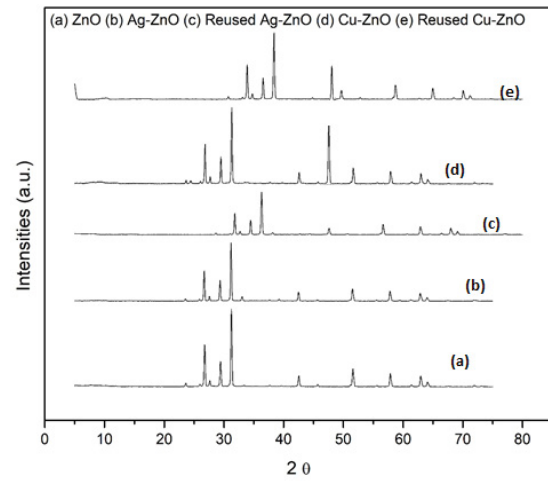

Fig. 4. XRD of (a) ZnO, (b) Ag-ZnO, (c) reused Ag-ZnO, (d) Cu-ZnO and (e) reused Cu-ZnO.
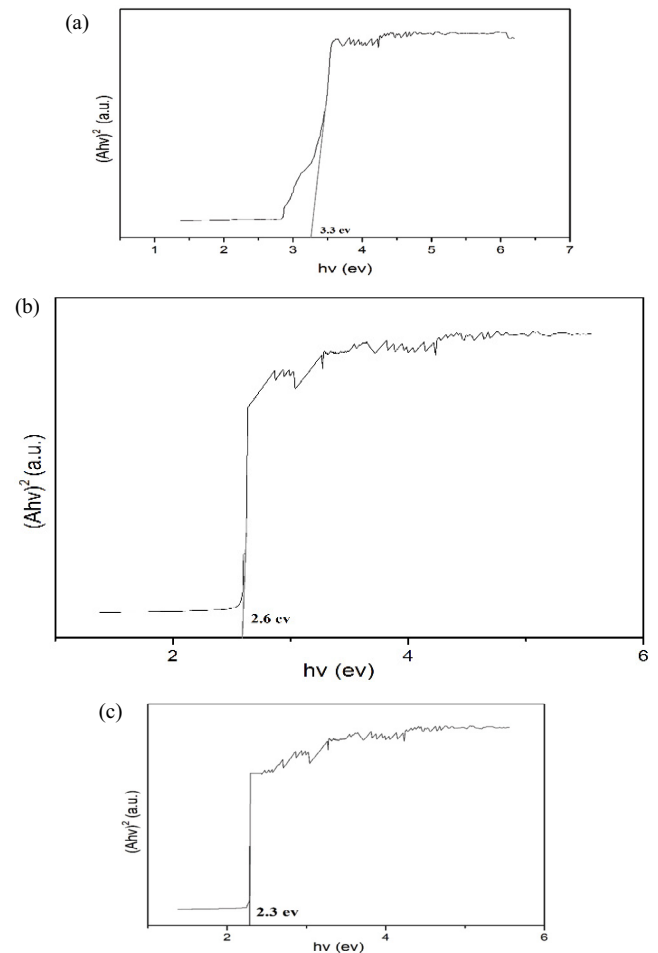

Fig. 5. Tauc plot for (a) ZnO, (b) Cu-ZnO and (c) Ag-ZnO.

sonophotocatalysis for 1 h with the own pH of drug, the weight of photocatalyst was also taken in a very low quantity, that is, 0.005 g and no oxidizing agents were used. Only 18.5% degradation of the drug was observed using Cu-ZnO.

It was found that low degradation of drug was observed during the photolysis and sonolysis, while it increased to 22.9%, 26.1% and 26.7% by using photocatalytic, sonocatalytic methods and sonophotocatalytic procedure respectively (Fig. 6).

3.3. pH effect

The effect of pH was studied in the range of pH 2–10 in the presence of Britton Robinson buffer and pH 4–10 was found as the ideal pH for the degradation of cefpodoxime proxetil. The degradation of cefpodoxime proxetil was 93.4% using Cu-ZnO as photocatalyst while it was 94.3% using Ag-ZnO (Fig. 7). pH, photocatalyst and ultrasonic waves had a significant effect on the degradation of cefpodoxime proxetil. As the alkaline pH increases the negative charge on the surface of cefpodoxime proxetil, making it very reactive to be attacked by a strong electrophile OH•. As well as the amide linkage and ester linkage present in cefpodoxime proxetil broken down in basic medium, which results in the rapid degradation of cefpodoxime proxetil. The point of zero charge of Cu-ZnO catalyst were determined and found pH 9 Cu-ZnO and Ag-ZnO was pH 8. The surface of catalyst is positively charged below pH 9 and 8 and negatively charged above pH 9 and 8. At pH higher than point of zero charge, the surface of catalyst is negatively charged and below it is positively charge,

electrostatic attraction between the positive charged catalyst and anionic dye occurred, which enhances the rate of OH• radicals' production. Increase in pH also results increase in the formation of OH• radicals. Cefpodoxime proxetil degradation also occurred in acidic pH, it may be because of the hydrolysis of the ester linkage (Fig. 7).

3.4. Time effect

For investigation of optimum time for maximum degradation the reaction time was varied from 10 to 100 min with 10 min interval in each case and 30 min was found as optimum for the degradation of cefpodoxime proxetil using Cu-ZnO and Ag-ZnO. Beyond 30 min time no increase in degradation was observed up to 100 min, therefore for subsequent studies, 30 min were used (Fig. 8).

3.5. Enhancer's effect

Various oxidants, such as hydrogen peroxide, sodium perchlorate and potassium peroxydisulfate, have been studied as activators of the sonophotocatalytic degradation of cefpodoxime proxetil. Reactions of the hydroxyl radicals are given in Eqs. (3)–(9) and mechanism was also published by many researchers [37,38]. As these hydroxyl radicals are very reacive and they are responcible for the degradation of dye by attacking on various positions on dye molecule.

$$Ag\text{-}ZnO + h\nu \rightarrow Ag\text{-}ZnO\left(h^+ + e^-\right) \tag{3}$$

$$H_2O_2 + h\nu\,/\,us \rightarrow OH^\bullet + H^+ \tag{4}$$

$$H_2O + h\nu\,/\,us \rightarrow OH^- + H^+ \tag{5}$$

$$OH^- + h^+ \rightarrow OH^\bullet \tag{6}$$

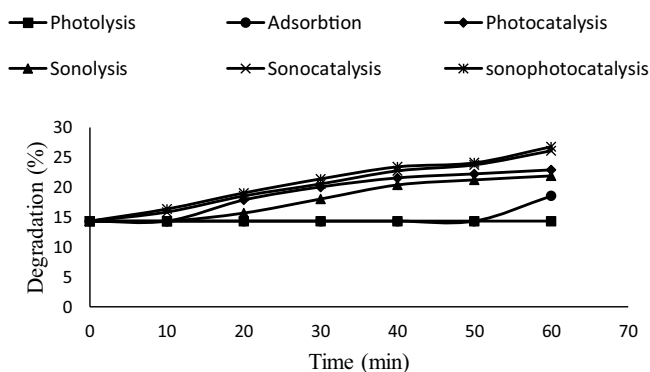$$OH^\bullet + \text{Cefpodoxime Proxetil} \rightarrow CO_2 + H_2O \tag{7}$$

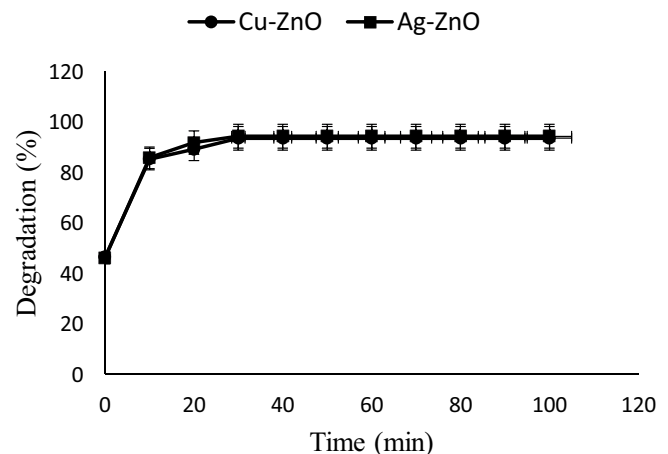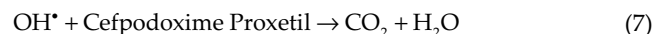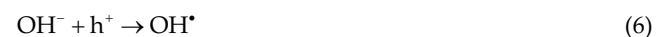Fig. 6. Degradation of cefpodoxime proxetil under different catalytic conditions at different time (min).
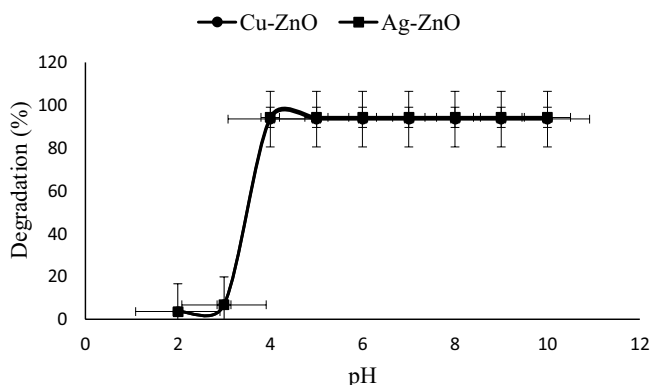
Fig. 7. Degradation of cefpodoxime proxetil at different pH using Cu-ZnO and Ag-ZnO as a photocatalyst.
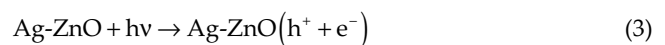

Fig. 8. Degradation of cefpodoxime proxetil using different time with Cu-ZnO and Ag-ZnO as a photocatalyst.

$$O_2 + e^- \rightarrow {}^\bullet O_2^- \tag{8}$$

$$O_2 + \text{Cefpodoxime Proxetil} \rightarrow CO_2 + H_2O \tag{9}$$
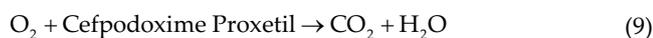
Sodium perchlorate effect on the degradation of drug is due to capturing the electron which generated on the photocatalyst conduction band [Eq. (10)] [39].

$$ClO_4^- + 8e^- + 8H^+ \rightarrow Cl^- + 4H_2O \tag{10}$$

Potassium peroxydisulphate as an enhancer also increase the degradation of drug due to formation of sulphate radicals, which react with water and form $OH^\bullet$ radicals [Eqs. (11)–(14)] [40].

$$S_2O_8^{2-} + h\nu \rightarrow 2SO_4^{\bullet-} \tag{11}$$

$$SO_4^{\bullet-} + H_2O \rightarrow SO_4^{2-} + OH^\bullet + H^+ \tag{12}$$

$$SO_4^{\bullet-} + \text{Cefpodoxime Proxetil} \rightarrow SO_4^{2-} + \text{drug} + H^+ \tag{13}$$

$$SO_4^{\bullet-} + \text{Cefpodoxime Proxetil} \rightarrow SO_4^{2-} + CO_2 + H_2O + \text{other inorganics} \tag{14}$$
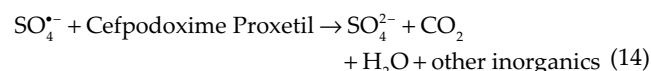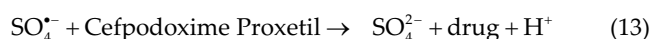
Using Cu-ZnO and Ag-ZnO as photocatalyst at neutral pH, catalyst dose = 0.05 g L^{-1} and the initial drug concentration 10 mg L^{-1} with reaction time of 30 min. The concentration of each activator ranged from 3 mmol to 8 mmol. The degradation of cefpodoxime proxetil increased from 86.2% to 99% with 8 mmol of hydrogen peroxide and competent to 92.3% with 8 mmol of sodium perchlorate and up to 87.2% with 8 mmol of potassium peroxydisulfate, respectively, using Cu-ZnO as photocatalyst. Whereas in the case of the degradation of Ag-ZnO, it increased to 99.7% with 5 mmol of hydrogen peroxide adequate for 92.3% and 90.6% using 8 mmol of sodium perchlorate and of potassium peroxydisulfate respectively (Fig. 9). Cefpodoxime proxetil mineralization was also confirmed using TOC analysis. The experimental conditions to performed TOC were 10 mg L^{-1} drug using 8 mmole of hydrogen peroxide at neutral pH for time of 2 h and catalyst dosage of 0.1 g L^{-1} of Cu-ZnO and 0.04 g L^{-1} of Ag-ZnO, under tungsten filament lamp (200 W). The % removal of TOC before and after the degradation were calculated and it was found 89% and 93% removal using Cu-ZnO and Ag-ZnO, which confirms the free radical mechanism of reaction also.

3.6. Catalyst dosage effect

The effect of catalyst dosage on the degradation of cefpodoxime proxetil was studied to improve the cost efficiency of the sonophotocatalytic degradation process. The weight of catalyst was varied in the range of 0.01–0.3 g L^{-1} at neutral pH using 10 mg L^{-1} drug concentration and 8 mmol of hydrogen peroxide (Fig. 10). It was observed
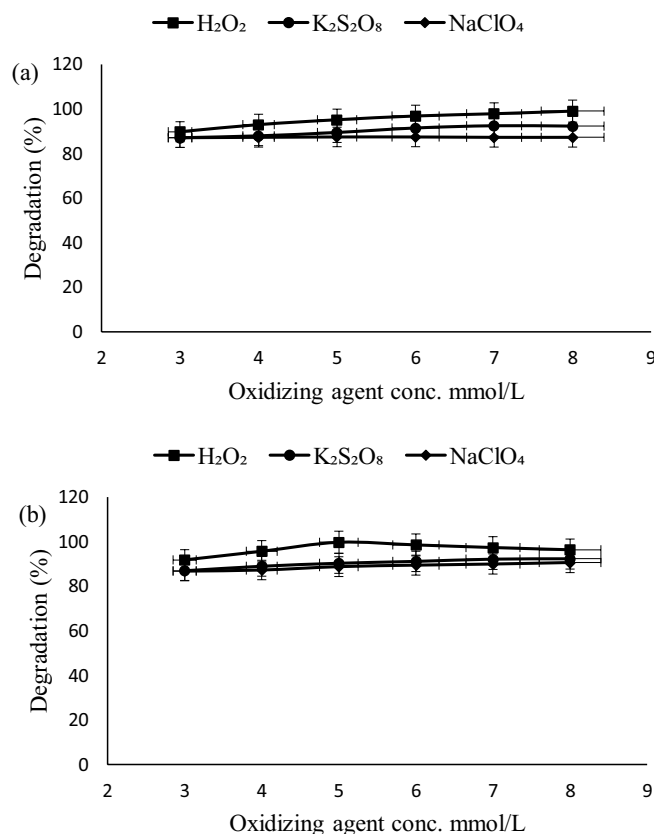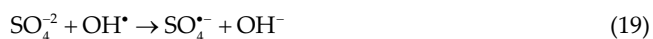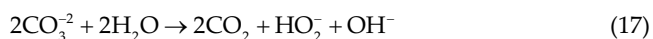

Fig. 9. Degradation of cefpodoxime proxetil at different mmol L^{-1} of oxidizing agents using Cu-ZnO and Ag-ZnO as a photocatalysts.

that with increasing weight of catalyst (0.01 to 0.1 g L^{-1} using Cu-ZnO and 0.01 to 0.04 g L^{-1} using Ag-ZnO) there was an increase in degradation of cefpodoxime proxetil. Maximum degradation, that is, 100% was achieved with 0.1 g L^{-1} of Cu-ZnO and 0.04 g L^{-1} of Ag-ZnO. A further increase in the weight of catalyst leads to a decrease in the degradation of cefpodoxime proxetil. This may be due to aggregation of the catalyst particles in solution, resulting in a decrease of the active sites of the catalyst for the generation of $OH^\bullet$ radicals. In addition, an excessive amount of catalyst leads to light scattering and, in turn, reduces the speed of the degradation process. In addition, it also leads to a decrease in the transparency of the solution that prevents the penetration of radiation.

3.7. Scavenger's effect

Keeping in view the potential application of the method to environmental samples, the effect of scavenger's has also been studied. Three different types of scavengers, such as chlorides, sulphates, and carbonates, have been studied for the degradation of cefpodoxime proxetil. The possible reaction that may occur is shown in Eqs. (15)–(19) [41].

$$Cl^- + OH^{\bullet-} \rightarrow Cl^\bullet + OH^- \tag{15}$$

$$CO_3^{-2} + OH^\bullet \rightarrow CO_3^{\bullet-} + OH^- \tag{16}$$

$$2CO_3^{-2} + 2H_2O \rightarrow 2CO_2 + HO_2^- + OH^- \qquad (17)$$

$$OOH^- + OH^\bullet \rightarrow OH^- + OOH^\bullet \qquad (18)$$

$$SO_4^{-2} + OH^\bullet \rightarrow SO_4^{\bullet-} + OH^- \qquad (19)$$

The concentration of scavenger's was kept constant, that is, 0.1 M. It was observed that the presence of these anions reduces the effectiveness of the degradation of cefpodoxime proxetil. The decreasing efficiency of chlorides was greater than that of carbonates and sulphates. Chloride anions reduce the efficiency of degradation up to 63.5%, carbonates down to 71.9% and sulphates up to 70.3% (Fig. 11).

3.8. Effect of initial drug concentration

For the preliminary investigation and optimization of various parameters we used 10 ppm concentration of selected pollutant due to its discharge after reaction, but when all the parameters were optimized effect of concentration
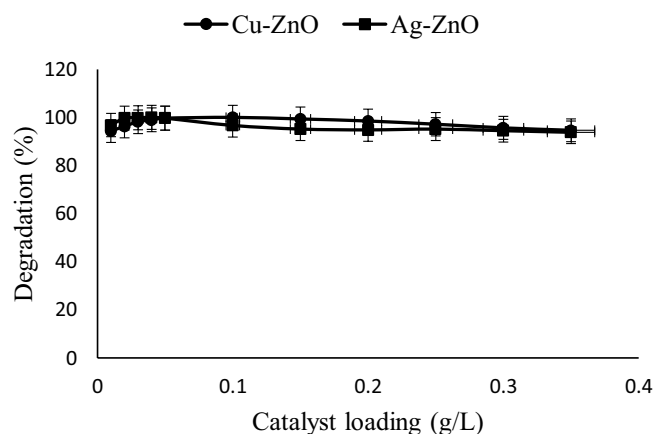

Fig. 10. Degradation of cefpodoxime proxetil using different weight of catalysts (Cu-ZnO) and (Ag-ZnO).
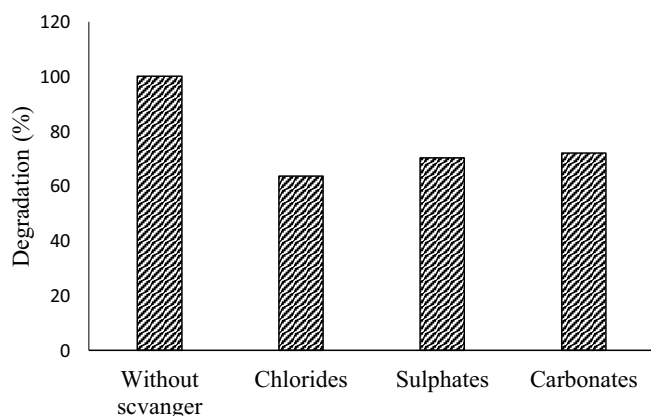

Fig. 11. Effect of scavenger on the degradation of cefpodoxime proxetil.

was checked to 100 ppm. Effect of the initial concentration of cefpodoxime proxetil was investigated for sonophotocatalytic degradation in the range of 10 to 100 mg L^{-1}. It was found that for 10 mg mL^{-1} at neutral pH, the catalyst dose for Cu-ZnO = 0.1 g L^{-1}, Ag-ZnO = 0.04 g L^{-1}, 8 mmol hydrogen peroxide, 100% degradation of cefpodoxime proxetil was obtained using Cu-ZnO and Ag-ZnO as photocatalyst. The percent degradation of the drug decreased with increasing initial concentration. It decreased from 100% to 90.8% with 10 mg L^{-1} for Cu-ZnO and from 100% to 95.1% with 10 mg L^{-1} using Ag-ZnO as photocatalyst (Fig. 12).

3.9. Catalyst reusability

The reuse of the catalyst is important to evaluate its practical utility. For reuse, the sonophotocatalytic activity of photocatalysts Cu-ZnO and Ag-ZnO were studied after successive uses. For the degradation of cefpodoxime proxetil, the catalyst was collected by centrifugation and washed with different polar organic solvents (ethanol, methanol, acetone, and acetonitrile) and then with distilled water. The effect of the solvents used to wash the catalyst was the same because of the solubility of the adsorbed drug on the organic solvents. Therefore, ethanol was chosen due to low cost, easy availability and safety for subsequent catalyst washing. After drying, the catalyst was again used with a fresh drug solution under optimized degradation conditions. In the case of Cu-ZnO, the degradation decreased from 100% to 99% and increased the degradation time, whereas in Ag-ZnO, the degradation efficiency decreases to 99.3% (Fig. S1).

3.10. Sample application

The proposed sonophotocatalytic method was applied to the synthetic cefpodoxime proxetil sample. The sonophotocatalytic degradation of the samples was performed under optimized conditions of pH, H$_2$O$_2$, catalyst weight and degradation were calculated for each photocatalyst. It was observed that the synthetic cefpodoxime proxetil sample was degraded up to 99% using Cu-ZnO and 98.8% using Ag-ZnO as a photocatalyst with 60 min reaction time (Fig. 13).
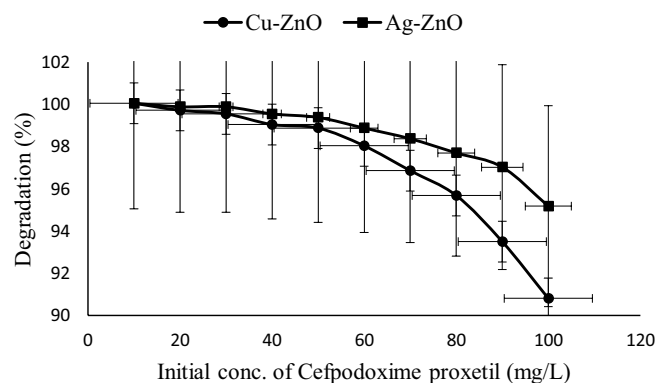

Fig. 12. Degradation of cefpodoxime proxetil at different initial drug concentration (mg/mL) using (Cu-ZnO) and (Ag-ZnO) photocatalyst.

3.11. Kinetic models

For the kinetics of the sonophotocatalytic degradation of cefpodoxime proxetil was performed, and the rate constants were determined by the different kinetic models [42].

A linear plot of $\log(q_e - q_t)$ against t was plotted to determine the rate constant and degradation efficiency for pseudo-first-order for Cu-ZnO and Ag-ZnO (Fig. 15) and pseudo-second-order kinetic model for Cu-ZnO and Ag-ZnO (Fig. S2). The sonophotocatalytic degradation of cefpodoxime proxetil using Cu-ZnO and Ag-ZnO followed pseudo-first-order kinetic and the rate of degradation of cefpodoxime proxetil using Ag-ZnO is higher ($k_1 = 0.228$ min^{-1}) than the Cu-ZnO photocatalyst ($k_1 = 0.185$ min^{-1}) (Table S1).

3.12. Adsorption isotherms

Two different adsorption isotherms were applied, that is, Freundlich adsorption isotherm and Langmuir adsorption isotherm. Freundlich based on heterogeneous surface of the adsorbent and therefore responsible for multilayer adsorption due to the process of energetically heterogeneous adsorption sites. Freundlich adsorption isotherm for photocatalysts was drawn by plotting $\log q_e$ vs. $\log C_e$ as shown
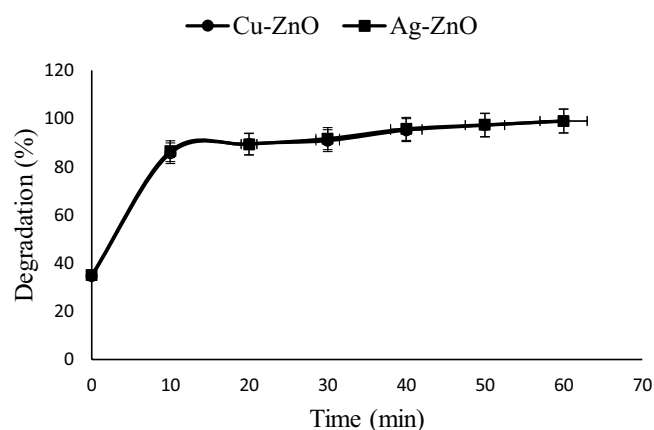

Fig. 13. Application of sonophotocatalytic method for the degradation of synthetic sample.
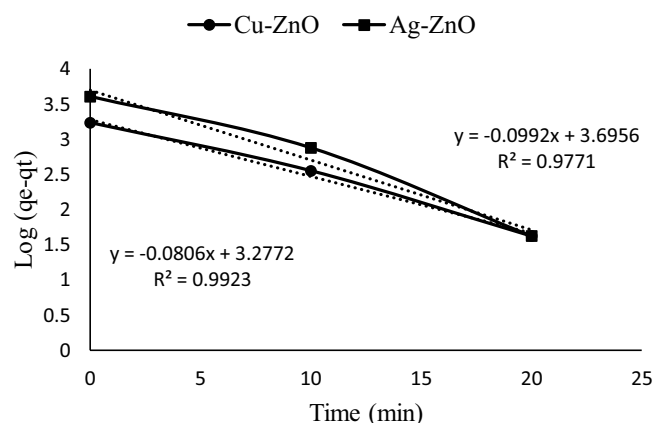

Fig. 14. Pseudo-first-order kinetic model for cefpodoxime proxetil using (Cu-ZnO) and (Ag-ZnO) photocatalyst.

in figure. It was observed that proposed degradation followed Langmuir adsorption isotherm as Langmuir model assumes that the surface of photocatalyst is heterogeneous and a monomolecular layer is formed when adsorption takes place without any interaction between adsorbed molecules. Langmuir adsorption isotherm was drawn by plotting C_e/q_e vs. C_e as in figure. It can be concluded from the correlation coefficient R^2 value that the experimental data in accordance with the Langmuir isotherm (Fig. S3) better than the Freundlich adsorption isotherm (Fig. S4) for both the photocatalysts. This proves that cefpodoxime proxetil adsorption onto Cu-ZnO and Ag-ZnO adsorbate is almost homogeneously distributed on the surface of the adsorbent resulting in monolayer adsorption.

3.13. Comparison with other methods

The proposed method according to which the sonophotocatalytic degradation of cefpodoxime proxetil using Cu-ZnO and Ag-ZnO photocatalysts has been compared to other methods using different irradiation sources and photocatalysts in the literature is presented in Table 2 and it was found that our proposed sonophotocatalytic technique is superior to the other proposed degradation methods.

3.13.1. Plausible degradation mechanism

The plausible degradation mechanism for the sonophotocatalytic degradation of cefixime proxetil are given in Figs. S5 and S6 and follows three different ways, that is, sono-luminescence, hot spot, and oxygen atom escape. As ultrasonic radiations overcome the drawbacks of conventional methods like it reduces the chances of agglomeration of nanoparticles by continually dispersion as well as increases surface to volume ratio by continuously refreshing the surface of catalyst by ultrasonic radiations and enhances mass transfer improvement because of active site increasement [42]. Moreover, in emission and formation of hotspot leads to dissociation of water molecules which further causes the formation of free radicals and enhancement of oxygen molecules leads to the degradation of cefpodoxime proxetil.

3.13.2. Nucleation

The physical phenomenon of ultrasonic radiations, that is, cavitation bubbles lead to the rapid expansion over the compression/rarefaction cycles and these bubbles when reached to a critical size result in sono-luminescence (SL) upon violent implosions in the liquid medium. SL consist of light emitting from 200–700 nm which further increases the electron hole pair formation results in generation of free radicals. Furthermore, chemical generation of HO$^{\bullet}$, HO$_2^{\bullet}$ and H$_2$O$_2$ free radicals from hot spot as well as electron hole pair from SL react with cefpodoxime proxetil and heat energy from hot spot could participate in excitement of sonocatalyst to form electron hole pairs and generation of more free oxidizing radicals subsequently [43]. Photocatalysis also results in the formation of electron hole pair which results in the formation of free hydroxyl radicals. All the reactive species produced from different physical and chemical phenomenon's taking place in a reaction

Table 2
Comparison of the proposed degradation method with other degradation methods used for different pharmaceuticals

No.	Drug	Degradation source for	Results and comments	Matrix	References
1.	Paracetamol	UV Lamp/H_2O_2	Complete degradation with mineralization degree upto 40%	Bi-distilled water	[44]
2.	Diclofenac	UV Lamp/H_2O_2	H_2O_2/UV system is effective in inducing diclofenac degradation at 90 min of treatment	Water solution	[45]
3.	Metronidazole	UV Lamp/H_2O_2	Degradation follows first-order kinetics and rate increases with increasing H_2O_2 concentration	Deionized water	[46]
4.	Naproxen, Ketoprofen, Carbamazepine, Clofibric acid, Ciprofloxacin, and Iohexol	UV Lamp/H_2O_2	Complete degradation at 1,700 mJ cm^{-2} fluorescence for all drugs. Lower degradation with direct photolysis. Rates decrease in surface water compared with laboratory water	Laboratory grade water	[47]
5.	Ibuprofen, Diphenhydramine, Phenazone, and Phenytoin	UV Lamp/H_2O_2	UV/H_2O_2 advanced oxidation experiments were effective for selected drugs	Deionized water	[48]
6.	Meprobamate, Carbamazepine, Dilantin, Atenolol, Primidone, and Trimethoprim	UV Lamp/H_2O_2	Removal of the six pharmaceuticals varied between no observed removal and >90%	Wastewater effluents	[49]
7.	11 pharmaceuticals	UV Lamp/H_2O_2	UV/H_2O_2 generally appeared to be a more efficient technology for removing pharmaceuticals from RO brines	Reclamation osmosis brines	[50]
8.	Clofibric acid	UV Lamp/H_2O_2	Almost complete removal of clofibric acid in 60 min with low concentration	Aqueous solution	[51]
9.	Cefpodoxime proxetil	Ultrasonic waves with Tungsten Lamp (100 W)	100% degradation was obtained at pH 4–10 using Cu-ZnO.	Aqueous solution	Present work
10	Cefpodoxime proxetil	Ultrasonic waves with Tungsten Lamp (100 W)	100% degradation was obtained at pH 4–10 using Ag-ZnO catalyst	Aqueous solution	Present work

chamber react with cefpodoxime proxetil and convert it into H_2O, CO_2 and different mineral acids.

4. Conclusion

A comparative study of Cu-impregnated ZnO and Ag-impregnated ZnO for the sonophotocatalytic degradation of cefpodoxime proxetil in aqueous solution under visible light irradiation was conducted. pH 4–10 was found to be the ideal pH for cefpodoxime proxetil due to which cefpodoxime proxetil can be degraded in effluent directly in 30 min. A degradation efficiency of 100% for cefpodoxime proxetil was obtained at optimum conditions for Cu-ZnO and Ag-ZnO catalyst. The results of photocatalysts reusability were very good up to third cycle of reuse. The scavenger's study shows that the decreasing efficiency of chlorides was greater than that of carbonates and sulphates. Chloride anions reduce the efficiency of degradation from 100% up to 63.5%, carbonates up to 71.9% and sulphates 70.3%. The sonophotocatalytic degradation of cefpodoxime proxetil using Cu-ZnO and Ag-ZnO followed pseudo-first-order kinetic and the rate of degradation of cefpodoxime proxetil

using Ag-ZnO is higher (k_1 = 0.228) than the Cu-ZnO photocatalyst (k_1 = 0.185). The proposed sonophotocatytic method allows the analysis of pharmaceutical residues containing μg mL^{-1} levels of the test compound.

References

[1] A. Pourtaheri, A. Nezamzadeh-Ejhieh, Photocatalytic properties of incorporated NiO onto clinoptilolite nano-particles in the photodegradation process of aqueous solution of cefixime pharmaceutical capsule, Chem. Eng. Res. Des., 104 (2015) 835–843.

[2] N.M. Shooshtari, M.M. Ghazi, An investigation of the photocatalytic activity of nano α-Fe$_2$O$_3$/ZnO on the photodegradation of cefixime trihydrate, Chem. Eng. J., 315 (2017) 527–536.

[3] S. Sahraeian, V. Alipour, O. Rahmanian, High efficient degradation of cefixime using UV/TiO$_2$ photocatalytic process: a comparison between photocatalytic and photolytic, Hormozgan Med. J., 21 (2017) 159–168.

[4] A.O. Ebenezer, C. Chioma, I.M. Omoegbe, Instability of cefpodoxime proxetil oral suspension at different temperature storage conditions, J. Pharm. Pharm., 5 (2017) 1–6.

[5] D.W. Kolpin, E.T. Furlong, M.T. Meyer, E. Michael Thurman, S.D. Zaugg, L.B. Barber, H.T. Buxton, Pharmaceuticals, hormones, and other organic wastewater contaminants in

U. S. streams, 1999–2000: a national reconnaissance, Environ. Sci. Technol., 36 (2002) 1202–1211.

[6] M. Scheurell, S. Franke, R.M. Shah, H. Hühnerfuss, Occurrence of diclofenac and its metabolites in surface water and effluent samples from Karachi, Pakistan, Chemosphere, 77 (2009) 870–876.

[7] K.P. Henschel, A. Wenzel, M. Diedrich, A. Fliedner, Environmental hazard assessment of pharmaceuticals, Regul. Toxicol. Pharm., 25 (1997) 220–225.

[8] B. Halling-Sørensen, S. Nors Nielsen, P.F. Lanzky, F. Ingerslev, H.C. Holten Lützhøft, S.E. Jørgensen, Occurrence, fate and effects of pharmaceutical substances in the environment - a review, Chemosphere, 36 (1998) 357–393.

[9] K. Fent, A.A. Weston, D. Caminada, Ecotoxicology of human pharmaceuticals, Aquat. Toxicol., 76 (2006) 122–159.

[10] L.A. Al-Khateeb, S. Almotiry, M.A. Salam, Adsorption of pharmaceutical pollutants onto graphene nanoplatelets, Chem. Eng. J., 248 (2014) 191–199.

[11] H.A. Patehkhor, M. Fattahi, M. Khosravi-Nikou, Synthesis and characterization of ternary chitosan–TiO_2–ZnO over graphene for photocatalytic degradation of tetracycline from pharmaceutical wastewater, Sci. Rep., 11 (2021) 24177, doi: 10.1038/s41598-021-03492-5.

[12] R. Noroozi, M. Gholami, M. Farzadkia, R.R. Kalantary, Synthesis of new hybrid composite based on TiO2 for photocatalytic degradation of sulfamethoxazole and pharmaceutical wastewater, optimization, performance, and reaction mechanism studies, Environ. Sci. Pollut. Res., (2022), doi: 10.1007/s11356-022-19375-9 (In Press).

[13] L.-L. He, X.-Y. Li, J.-Y. Bai, S. Li, S. Qi, X. Wang, Y. Li, A novel ZnWO4/MgWO4 n-n heterojunction with enhanced sonocatalytic performance for the removal of methylene blue: characterizations and sonocatalytic mechanism, Surf. Interfaces, (2022) 101980, doi: 10.1016/j.surfin.2022.101980.

[14] J. Shah, M.R. Jan, F. Khitab, Sonophotocatalytic degradation of textile dyes over Cu-impregnated ZnO catalyst in aqueous solution, Process Saf. Environ. Prot., 116 (2018) 149–158.

[15] F. Khitab, M.R. Jan, J. Shah, Sonophotocatalytic degradation of aqueous Acid Red 27 and Direct Violet 51 using copper impregnated Al_2O_3, Desal. Water Treat., 137 (2019) 381–394.

[16] F. Khitab, M.R. Jan, J. Shah, Removal of hazardous textile dyes from water using Ni impregnated ZnO through sonophotocatalytic degradation, Desal. Water Treat., 205 (2020) 357–372.

[17] W. Baran, A. Makowski, W. Wardas, The effect of UV radiation absorption of cationic and anionic dye solutions on their photocatalytic degradation in the presence TiO_2, Dyes Pigm., 76 (2008) 226–230.

[18] N. Daneshvar, M. Rabbani, N. Modirshahla, M.A. Behnajady, Photooxidative degradation of Acid Red 27 in a tubular continuous-flow photoreactor: influence of operational parameters and mineralization products, J. Hazard. Mater., 118 (2005) 155–160.

[19] S. Dolatabadi, M. Fattahi, M. Nabati, Solid state dispersion and hydrothermal synthesis, characterization and evaluations of TiO_2/ZnO nanostructures for degradation of Rhodamine B, Desal. Water Treat., 231 (2021) 425–435.

[20] H. Mahmoodi, M. Fattahi, M. Motevassel, Graphene oxide–chitosan hydrogel for adsorptive removal of diclofenac from aqueous solution: preparation, characterization, kinetic and thermodynamic modelling, RSC Adv., 11 (2021) 36289–36304.

[21] A.A. Isari, S. Moradi, S.S. Rezaei, F. Ghanbari, E. Dehghanifard, B. Kakavandi, Peroxymonosulfate catalyzed by core/shell magnetic ZnO photocatalyst towards malathion degradation: enhancing synergy, catalytic performance and mechanism, Sep. Purif. Technol., 275 (2021) 119163, doi: 10.1016/j.seppur.2021.119163.

[22] M. Moradi, F. Hasanvandian, A. Akbar Isari, F. Hayati, B. Kakavandi, S.R. Setayesh, CuO and ZnO co-anchored on g-C_3N_4 nanosheets as an affordable double Z-scheme nanocomposite for photocatalytic decontamination of amoxicillin, Appl. Catal., B, 285 (2021) 119838, doi: 10.1016/j.apcatb.2020.119838.

[23] S. Moradi, S.A. Sobhgol, F. Hayati, A. Akbar Isari, B. Kakavandi, P. Bashardoust, B. Anvaripour, Performance and reaction mechanism of MgO/ZnO/Graphene ternary nanocomposite in coupling with LED and ultrasound waves for the degradation of sulfamethoxazole and pharmaceutical wastewater, Sep. Purif. Technol., 251 (2020) 117373, doi: 10.1016/j.seppur.2020.117373.

[24] X. Zhou, Y. Li, T. Peng, W. Xie, X. Zhao, Synthesis, characterization and its visible-light-induced photocatalytic property of carbon doped ZnO, Mater. Lett., 63 (2009) 1747–1749.

[25] M. Ahmad, E. Ahmed, Y. Zhang, N.R. Khalid, J. Xu, M. Ullah, Z. Hong, Preparation of highly efficient Al-doped ZnO photocatalyst by combustion synthesis, Curr. Appl. Phys., 13 (2013) 697–704.

[26] M. Ahmad, E. Ahmed, F. Zafar, N.R. Khalid, N.A. Niaz, A. Hafeez, M. Ikram, M. Ajmal Khan, Z. Hong, Enhanced photocatalytic activity of Ce-doped ZnO nanopowders synthesized by combustion method, J. Rare Earths, 33 (2015) 255–262.

[27] E. Regulska, J. Breczko, A. Basa, A.T. Dublis, Rare-earth metals-doped nickel aluminate spinels for photocatalytic degradation of organic pollutants, Catalysts, 10 (2020) 1003, doi: 10.3390/catal10091003.

[28] A. Khataee, R.D.C. Soltani, A. Karimi, S.W. Joo, Sonocatalytic degradation of a textile dye over Gd-doped ZnO nanoparticles synthesized through sonochemical process, Ultrason. Sonochem., 23 (2015) 219–230.

[29] A. Khataee, S. Saadi, M. Safarpour, S.W. Joo, Sonocatalytic performance of Er-doped ZnO for degradation of a textile dye, Ultrason. Sonochem., 27 (2015) 379–388.

[30] S. Anandan, A. Vinu, K.L.P. Sheeja Lovely, N. Gokulakrishnan, P. Srinivasu, T. Mori, V. Murugesan, V. Sivamurugan, K. Ariga, Photocatalytic activity of La-doped ZnO for the degradation of monocrotophos in aqueous suspension, J. Mol. Catal. A: Chem., 266 (2007) 149–157.

[31] P. Saharan, G.R. Chaudhary, S. Lata, S.K. Mehta, S. Mor, Ultra fast and effective treatment of dyes from water with the synergistic effect of Ni doped ZnO nanoparticles and ultrasonication, Ultrason. Sonochem., 22 (2015) 317–325.

[32] S. Chakma, V.S. Moholkar, Investigation in mechanistic issues of sonocatalysis and sonophotocatalysis using pure and doped photocatalysts, Ultrason. Sonochem., 22 (2015) 287–299.

[33] R. Ullah, J. Dutta, Photocatalytic degradation of organic dyes with manganese-doped ZnO nanoparticles, J. Hazard. Mater., 156 (2008) 194–200.

[34] A. Hezam, K. Namratha, Q.A. Drmosh, Z.H. Yamani, K. Byrappa, Synthesis of heterostructured Bi_2O_3–CeO_2–ZnO photocatalyst with enhanced sunlight photocatalytic activity, Ceram. Int., 43 (2017) 5292–5301.

[35] R. Saravanan, S. Karthikeyan, V.K. Gupta, G. Sekaran, V. Narayanan, A. Stephen, Enhanced photocatalytic activity of ZnO/CuO nanocomposite for the degradation of textile dye on visible light illumination, Mater. Sci. Eng., C, 33 (2013) 91–98.

[36] F. Khitab, J. Shah, M.R. Jan, Systematic assessment of visible light driven photocatalysts for the removal of cefixime in aqueous solution sonophotocatalytically, Int. J. Environ. Anal. Chem., (2021) 2025790, doi: 10.1080/03067319.2022.2025790.

[37] Y. Huang, G. Wang, H. Zhang, G. Li, D. Fang, Y. Song, Hydrothermal-precipitation preparation of CdS@(Er^{3+}:$Y_3Al_5O_{12}$/ZrO_2) coated composite and sonocatalytic degradation of caffeine, Ultrason. Sonochem., 37 (2017) 222–234.

[38] M. Qamar, M. Saquib, M. Muneer, Photocatalytic degradation of two selected dye derivatives, chromotrope 2B and amido black 10B, in aqueous suspensions of titanium dioxide, Dyes Pigm., 65 (2005) 1–9.

[39] U.I. Gaya, A.H. Abdullah, Heterogeneous photocatalytic degradation of organic contaminants over titanium dioxide: a review of fundamentals, progress and problems, J. Photochem. Photobiol., C, 9 (2008) 1–12.

[40] I.K. Konstantinou, T.A. Albanis, TiO_2-assisted photocatalytic degradation of azo dyes in aqueous solution: kinetic and mechanistic investigations: a review, Appl. Catal., B, 49 (2004) 1–14.

[41] A. Khataee, A. Karimi, S. Arefi-Oskoui, R.D.C. Soltani, Y. Hanifehpour, B. Soltani, S.W. Joo, Sonochemical synthesis of Pr-doped ZnO nanoparticles for sonocatalytic degradation of Acid Red 17, Ultrason. Sonochem. 22 (2015) 371–381.

[42] F. Hayati, M.R. Khodabakhshi, A.A. Isari, S. Moradi, B. Kakavandi, LED-assisted sonocatalysis of sulfathiazole and pharmaceutical wastewater using N,Fe co-doped TiO$_2$@SWCNT: optimization, performance and reaction mechanism studies, J. Water Process Eng., 38 (2020) 101693, doi: 10.1016/j.jwpe.2020.101693.

[43] S. Moradi, A.A. Isari, F. Hayati, R.R. Kalantary, B. Kakavandi, Co-implanting of TiO$_2$ and liquid-phase-delaminated g-C$_3$N$_4$ on multi-functional graphene nanobridges for enhancing photocatalytic degradation of acetaminophen, Chem. Eng. J., 414 (2021) 128618, doi: 10.1016/j.cej.2021.128618.

[44] R. Andreozzi, V. Caprio, R. Marotta, D. Vogna, Paracetamol oxidation from aqueous solutions by means of ozonation and H$_2$O$_2$/UV system, Water Res., 37 (2003) 993–1004.

[45] D. Vogna, R. Marotta, A. Napolitano, R. Andreozzi, M. d'Ischia, Advanced oxidation of the pharmaceutical drug diclofenac with UV/H$_2$O$_2$ and ozone, Water Res., 38 (2004) 414–422.

[46] H. Shemer, Y.K. Kunukcu, K.G. Linden, Degradation of the pharmaceutical metronidazole via UV, Fenton and photo-Fenton processes, Chemosphere, 63 (2006) 269–276.

[47] V.J. Pereira, H.S. Weinberg, K.G. Linden, P.C. Singer, UV degradation kinetics and modeling of pharmaceutical compounds in laboratory grade and surface water via direct and indirect photolysis at 254 nm, Environ. Sci. Technol., 41 (2007) 1682–1688.

[48] F. Yuan, C. Hu, X. Hu, J. Qu, M. Yang, Degradation of selected pharmaceuticals in aqueous solution with UV and UV/H$_2$O$_2$, Water Res., 43 (2009) 1766–1774.

[49] F.L. Rosario-Ortiz, E.C. Wert, S.A. Snyder, Evaluation of UV/H$_2$O$_2$ treatment for the oxidation of pharmaceuticals in wastewater, Water Res., 44 (2010) 1440–1448.

[50] A. Justo, O. González, J. Aceña, S. Pérez, D. Barceló, C. Sans, S. Esplugas, Pharmaceuticals and organic pollution mitigation in reclamation osmosis brines by UV/H$_2$O$_2$ and ozone, J. Hazard. Mater., 263 (2013) 268–274.

[51] R. Andreozzi, V. Caprio, R. Marotta, A. Radovnikovic, Ozonation and H$_2$O$_2$/UV treatment of clofibric acid in water: a kinetic investigation, J. Hazard. Mater., 103 (2003b) 233–246.
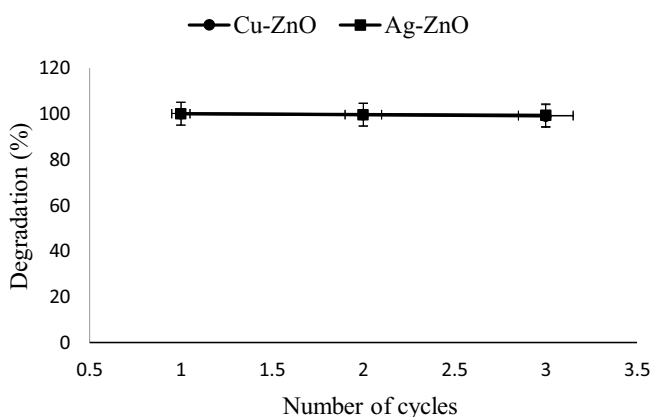
Supplementary information

Fig. S1. Degradation of cefpodoxime proxetil vs. reusability of (Cu-ZnO) and (Ag-ZnO) photocatalyst.

Table S1
Comparison of kinetic studies for the sonophotocatalytic degradation of cefpodoxime proxetil

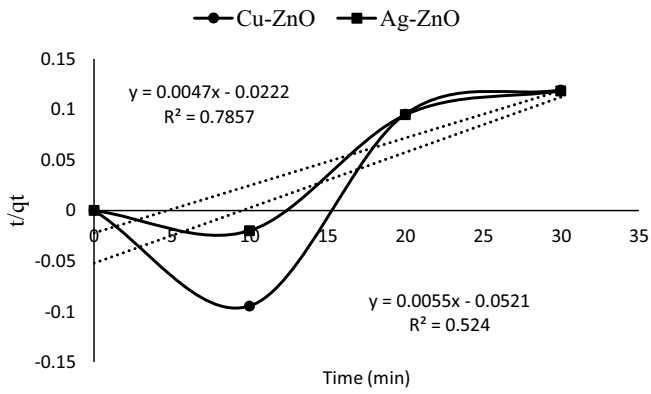| Catalyst	Pseudo-first-order				Pseudo-second-order		
	$q_{e(exp)}$ (mg g^{-1})	k_1 (min^{-1})	q_e (mg g^{-1})	R^2	k_2 (min^{-1})	q_e (mg g^{-1})	R^2
Cu-ZnO	0.251	0.185	1.892	0.992	$5.8 \times 10^{+4}$	0.181	0.524
Ag-ZnO	0.253	0.228	4.961	0.977	$4.2 \times 10^{+4}$	0.212	0.785

Fig. S2. Pseudo-second-order kinetic model for cefpodoxime proxetil using (Cu-ZnO) and (Ag-ZnO) photocatalyst.
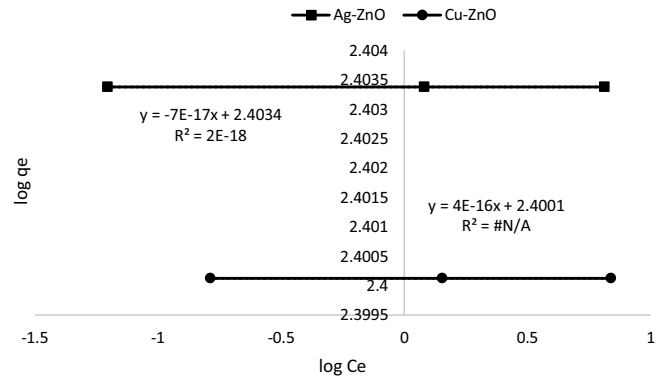

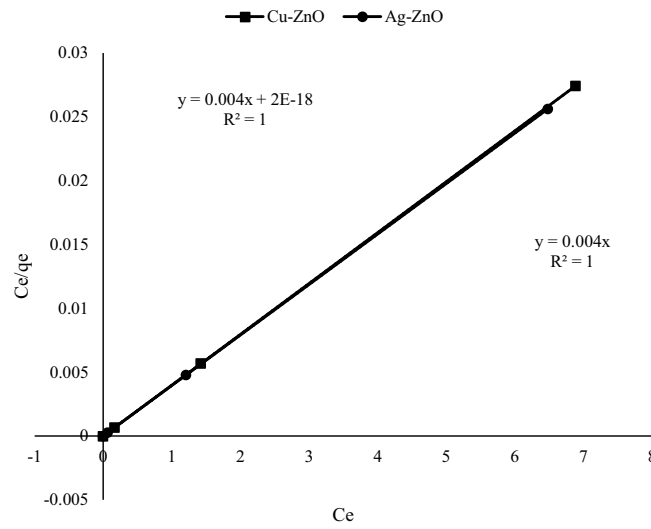Fig. S3. Freundlich adsorption isotherm for cefpodoxime proxetil.

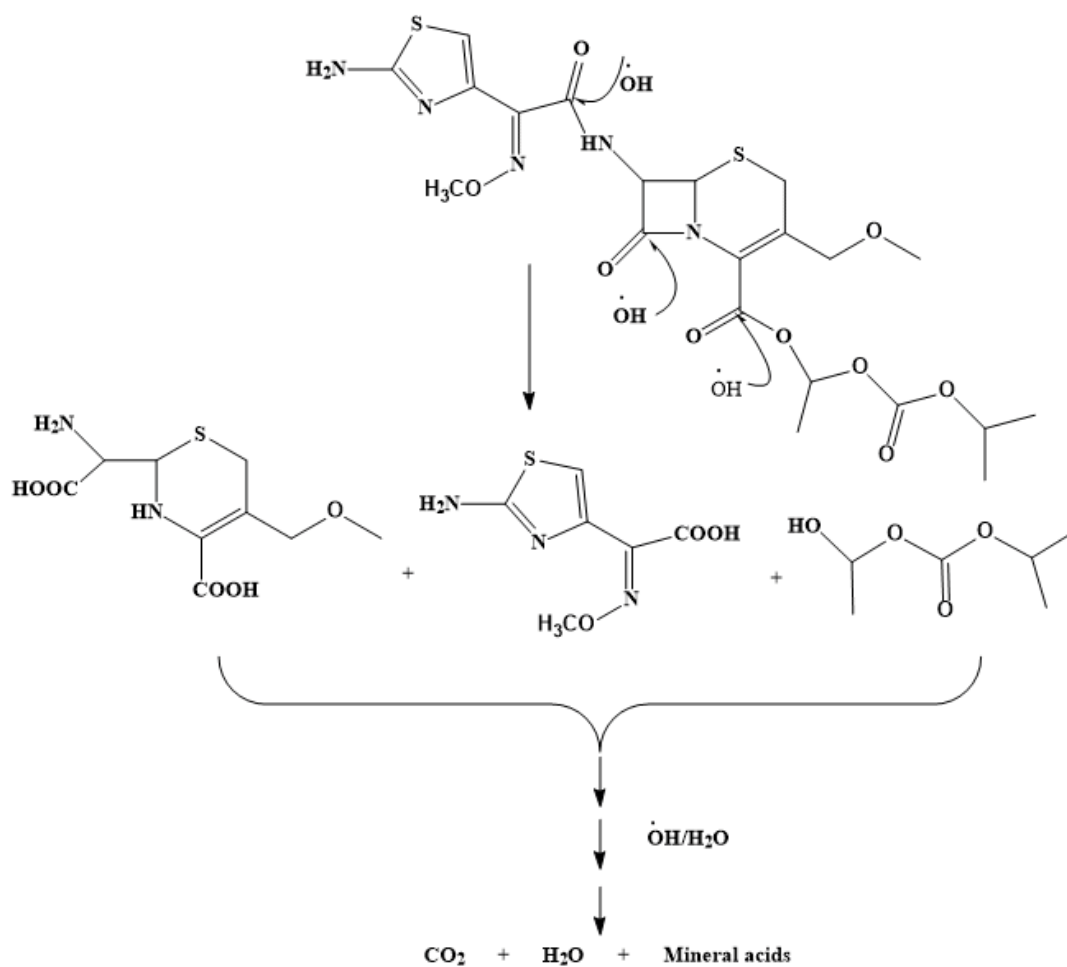Fig. S4. Langmuir isotherm for cefpodoxime proxetil.
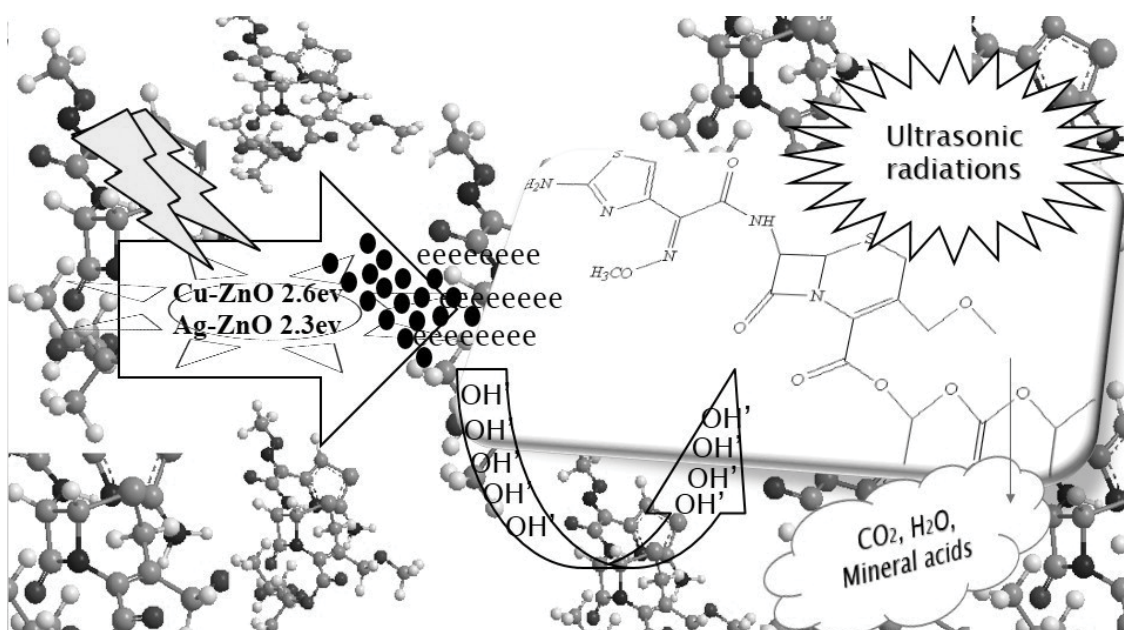
Fig. S5. Degradation mechanism of cefpodoxime proxetil.

Fig. S6. Graphical abstract for the degradation of cefpodoxime proxetil.